4M.3

CONVECTIVE AND OROGRAPHIC ASPECTS IN THE FORMATION OF A PRE–CYCLOGENIC AFRICAN EASTERLY WAVE NEAR THE ETHIOPIAN HIGHLANDS

Christopher M. Hill and Yuh-Lang Lin*
Department of Marine, Earth, and Atmospheric Sciences
North Carolina State University, Raleigh, North Carolina

1. Introduction

The African easterly wave (AEW) that would form the basis of Hurricane Alberto (2000) originated in the vicinity of the Ethiopian Highlands (EH) 5 days prior to cyclogenesis over the eastern Atlantic Ocean (Hill and Lin 2003, Lin et al. 2005). Initial convection began over the peaks of the northern EH during the local afternoon of 28 July 2000 (Fig. 1.1a). After dusk, the convective cells continued to grow as they tracked westward (Fig. 1.1b). By 2200 UTC 28 July 2000, growing convective cells from Eritrea moved southwestward and combined with westward-moving cells from northern Ethiopia, resulting in the development of an MCC (Fig. 1.1c). As the local nighttime progressed, the MCC peaked and began to diminish as it propagated in a southwestward and even southward direction (Fig. 1.1d). With the convection continuing to diminish, the overall cloud feature resumes a more westward track (Fig. 1.1e). From the residual clouds, a mesovortex (MV) becomes evident over central Sudan at 1600 UTC 29 July 2000 (Fig. 1.1f). From that time, the MV would continue westward and contribute to the generation of a larger MCC over southern Chad; the National Hurricane Center first recognized the AEW by this cloud signature in a post-mortem tropical cyclone report (Beven 2000).

The development of the incipient MCC from the EH is not unlike MCC development from the Rocky Mountains (Cotton et al. 1983, Wetzel et al. 1983). Convective cells initially develop over the higher mountain peaks and are advected to a region of lower elevation with high low-level moisture, which supplies the convection for further growth. An MCC later forms over the moisture rich region during the local nighttime. The important differences between the two scenarios of MCC development are in latitude, moisture availability, and the direction of moisture advection relative to MCC propagation (e.g. Laing and Fritsch 1993, 2000). According to the Rossby radius of deformation, as given by Cotton et al. (1989):

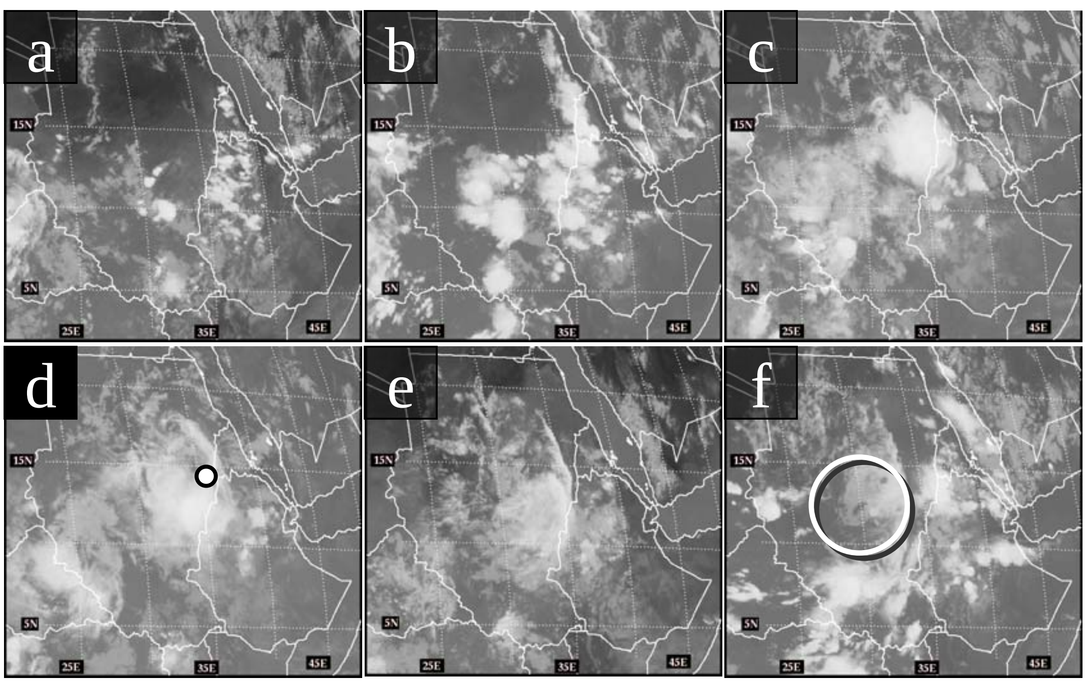

Fig. 1.1. METEOSAT-7 infrared-wavelength imagery for a) 1200 UTC 28 July 2000, b) 1600 UTC 28 July 2000, c) 2200 UTC 28 July 2000, d) 0400 UTC 29 July 2000, e) 1000 UTC 29 July 2000, and f) 1600 UTC 29 July 2000. Dot in d) depicts previous MCC center of c). Circle encompasses visible MV. Imagery provided by EUMETSAT © 2003.

* *Corresponding author address*: Dr. Yuh-Lang Lin, Dept. of MEAS, North Carolina State Univ., Campus Box 8208, Raleigh, NC 27695-8208. E-mail: yl_lin@ncsu.edu

$$\lambda_R = \frac{C_N}{(\zeta + f)^{\frac{1}{2}}\left(2VR^{-1} + f\right)^{\frac{1}{2}}},$$

where C_N is the phase speed of an inertia-gravity wave, ζ is the vertical component of relative vorticity, V is the tangential component of wind at the radius of curvature R, an MCC from the tropics can persist if it is sufficiently large or if it exhibits sufficiently strong internal rotation, such that $\lambda > \lambda_R$. The development of an MV allows the incipient MCC to persist for a time, and allows for future convective development near the MV (Fritsch et al. 1994, Trier et al. 2000a, b).

Existing theories may apply for the development of the MV, observed with the pre-Alberto AEW, involving the transition from the mature stage to the dissipating stage of the MCC. Within an MCC, an MV tends to form in conjunction with the stratiform precipitation region, above where relatively high CAPE and low vertical wind shear are conducive for MV development (Fritsch et al. 1994, among others). The MV with the pre-Alberto AEW likely arises from a cyclonic PV anomaly generated between a diabatically cooled surface-based layer and a diabatically warmed upper layer (Raymond and Jiang, 1990) within the intense convection.

A 3-day average of the 850-hPa mixing ratio and wind from ECMWF operational model data, surrounding the time of observed MCC development, shows the most significant advection of low-level moisture near the west slopes of the EH from the southwest (Fig. 1.2). Not only is moisture readily available for convective development over and to the west of the EH, the direction of moisture advection promotes leftward propagation of convective cells relative to the mean-layer (northeasterly) flow (Fig. 1.3), as occurred with the northernmost and most vigorous convection observed in the presented case.

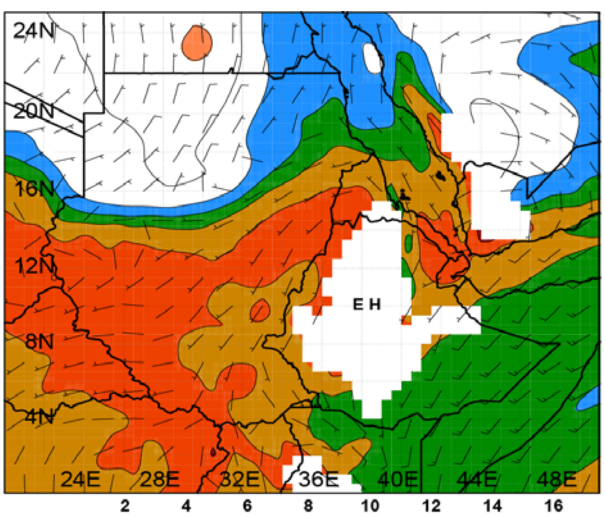

Fig. 1.2. ECMWF 3-day composite analysis of 850-hPa water vapor mixing ratio (g kg^{-1}) and wind (m s^{-1}) for 27 July to 29 July 2000. Contours every 2 g kg^{-1}.

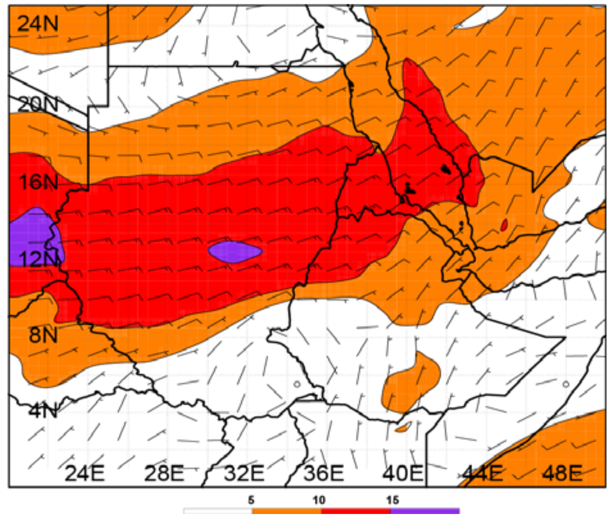

Fig. 1.3. ECMWF 3-day composite analysis of 600-hPa wind (m s^{-1}) for 27 July to 29 July 2000. Contours every 5 m s^{-1}.

The development of AEWs has largely been attributed to barotropic and baroclinic instabilities of the mid-tropospheric African Easterly Jet (Burpee 1972, Mass 1978, Thorncroft 1995), although AEW development has most always been described as taking place in central or west Africa. Furthermore, the instabilities associated with the AEJ provide the means for an AEW to be sustained or to grow, and not necessarily for its initiation. Carlson (1969) suggested that latent heating over significant terrain could be a mechanism for AEW generation. Being that the EH are a significant area of terrain located upstream of previously studied regions of AEW development, and being that strong convection took place over the EH for the case presented here, it stands to reason that an AEW could form near the EH.

A scarcity of observations has hindered study of AEW generation over east Africa. At best, global analyses show the synoptic patterns, and miss signals of AEW generation, in this region. Weigel and Herbster (1998) visited the idea of utilizing a mesoscale model study, and were apparently able to simulate an AEW from the EH region. The state of numerical weather simulation has reached the point where model output can serve as a proxy to missing observations. With this in mind, two non-hydrostatic mesoscale models are used here to simulate the environment surrounding the development of the "pre-Alberto" AEW. Primarily, the feasibility of simulating the generation of this AEW - and any other AEW - is tested.

The development of the initial mesoscale convective complex (MCC) and the associated mesovortex (MV), and a lee trough, are suggested to be crucial components to the generation of the AEW. A comparison of results from the two models is given here. The effects of orography, sensible heating, and latent heating on the convective and kinematic development of this AEW are examined.

2. Methodology

The non-hydrostatic Coupled Ocean-Atmosphere Meteorological Prediction System v.3, or COAMPS™ model (Chen et al. 2003), is used to simulate the environment of the area depicted in Fig. 2.1. The control simulation is conducted during the period of 00 UTC 27 July to 00 UTC 30 July 2000, during which time the incipient MCC is observed to develop, mature, and dissipate. The outer domain is set with 253 × 229 grid points spaced every 12 km, and the nested domain is set with 283 × 283 grid points spaced every 4 km. One-way nesting is employed, such that fields generated from the nested grid are not translated onto the coarse grid. The Kain-Fritsch cumulus parameterization (CP) scheme is used in the coarse (12-km) grid, and no CP scheme is used in the nested (4-km) grid. Vertically, each domain is structured with 42 σ-levels. The Rutledge-Hobbs microphysical parameterization (MP) scheme and a TKE-based boundary layer scheme are also employed. The domain boundaries are set with NOGAPS 12-hourly analyses of 1º grid spacing. The COAMPS model utilizes terrain data from the Global One-kilometer Base Elevation (GLOBE) Project.

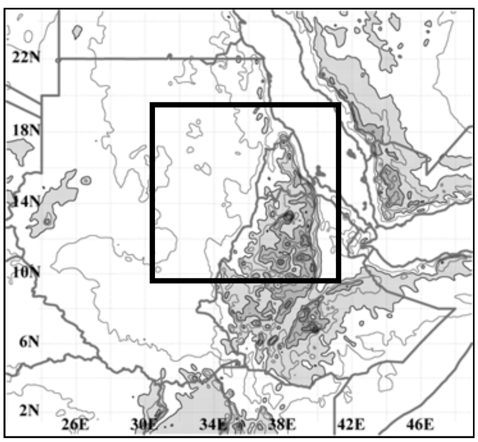

Fig. 2.1. GLOBE Project terrain (m) within the 12-km and 4-km spaced grids. Terrain is contoured every 500 m, and shaded every 1000 m above 1000 m.

The PSU/UCAR MM5 is also used to simulate the environment of the pre-Alberto AEW. The domain sizes are the same as with COAMPS model, yet the two domains of the MM5 are permitted to interact with one another through two-way nesting. Each domain is structured with 45 vertical σ-levels. The domain boundaries are set with ECMWF 6-hourly data with 1⅛º grid spacing. Again, the Kain-Fritsch CP scheme is used in the coarse grid, and no CP scheme is used in the nested grid. The Goddard MP scheme and the Blackadar PBL parameterization scheme are also employed with each domain of the MM5. The resolution of terrain data is 4 km for the coarse grid and 0.9 km for the nested grid.

Several sensitivity experiments are to be conducted: the reduced-terrain case (RT), no PBL case (NPBL), and no latent heating case (NLH). The RT simulations utilize a terrain field with height values half of those used in the CTRL simulations, and the new initial surface fields are extrapolated downward from the former initial surface fields. The NPBL case excludes surface fluxes and surface roughness. The NLH case excludes the CP and MP schemes.

3. Results

At 1200 UTC 28 July 2000, the hourly precipitation modeled by the MM5 more closely aligns with the initial convection observed in satellite imagery (Fig. 3.1a,b; compare with Fig. 1.1a). Over time, simulated precipitation increases and accumulates westward, following the convective elements over northern Ethiopia (Fig. 3.1c,d; Fig. 1.1b). Notably, the convection observed over Eritrea is not captured by either model. Near the time and place of the observed MCC peak, the precipitation from both models vanishes (Fig. 3.1e,f; Fig. 1.1c).

As the simulated initial convection protrudes through the easterly and northeasterly flow aloft, meso-β scale vorticity is generated near the convection and over the higher terrain of the EH (Fig. 3.2). As the convection expands and is advected westward, the areas of vorticity similarly grow and move (Fig. 3.3). By 2200 UTC 28 July 2000, a distinctive line of maximal vorticity along 37ºE represents a remnant wave from the convection (Fig. 3.4).

The convectively generated wave can be seen along 37ºE in a 700-hPa streamline field from the coarse domain at 2200 UTC 28 July 2000; additionally, a large cyclonic circulation is situated over southern Sudan (Fig. 3.5). The signals of these features are more prominent from the MM5. The cyclonic circulation over southern Sudan could be a lee trough; the development of this circulation may be analogous to lee vorticity development near the Central Mountain Range of Taiwan (Sun and Chern 1993, Lin et al. 1992), as well as near other topography of Africa (Mozer and Zehnder, 1996). By 0600 UTC 29 July 2000, the convectively generated wave from COAMPS lags, at 34ºE, behind the lee trough, while the wave from MM5 combines with the lee trough (Fig. 3.6). At this point, an AEW appears to have formed in the MM5 simulation.

Analysis of equivalent potential temperature (θ_e) from both models at 550 hPa (not shown) reveals that a region of low θ_e traverses the northern EH near the period of observed convective development. Cross-sectional analysis of MM5 equivalent potential temperature over Eritrea shows a surface layer of increasing θ_e over the higher peaks and plateau of the northern EH and beneath the traversing region of low θ_e (Fig. 3.7a); this phenomenon also occurs over northern Ethiopia. Although significant potential instability is present over Eritrea, simulated convection in this area is weak and short-lived (Fig. 3.7b); the potentially warm low layer remains trapped near the surface, as there apparently is no simulated trigger for intense convection.

The elevated heat source of the EH surface and the surrounding moisture sources of the Red Sea and the Congolese rain forests are shown to be crucial to the initiation of the scattered afternoon convection, and the eventual maturity of the convection into an MCC, with the no-sensible-heat-flux (NSH) and no-latent-heat-flux (NLH) experiments. The reduced-terrain (RT) experiment indicates that convection alone produces a weak wave signature, and that the true local orography contributes significantly to the development of the convection and of the pre-Alberto AEW.

4. Conclusions

The two mesoscale models employed were able to replicate, to an extent, some but not all of the convection associated with the developing pre-Alberto AEW. The MM5 gave a good representation of the initial convection over the peaks of EH. The difference of the two models in the representation of the initial convection could be attributed simply to the differences of the models themselves; the MM5 utilizes 6-hourly ECMWF data and two-way nesting. The fact that both models miss the pivotal convective development over Eritrea could be explained by inadequate model initialization. Despite the diminutive nature of the evolving precipitation field, a traceable wave was generated from the convection that was resolved. If the models could sufficiently capture the observed convection, a stronger wave and an MV may be produced from the simulations.

With satellite data being the only reliable observations, it is proposed that mesoscale numerical models provide the best existing means for examining mesoscale features leading to the generation of MCCs and AEWs near the EH region; in turn, satellite data best verifies the results of model simulations of the EH environment. Through a comparison between model results and with satellite data, the development of the pre-Alberto AEW appears to take place in four stages: 1) cellular convection develops in the local afternoon over the higher mountain peaks of the EH, 2) growing convective cells conglomerate into an MCC during the local nighttime near the lee slopes of the EH, 3) an MV develops from the remnants of the MCC, and 4) the convectively-generated MV combines with a pre-existing lee trough to form the AEW.

5. Future Work

More testing is needed to produce a more accurate simulation of the formation of the pre-Alberto AEW; finer grid resolution and the inclusion of a land surface model are possible approaches to this end. Additional model sensitivity experiments are planned to investigate more precisely the formation mechanisms for the pre-Alberto AEW. Smoothing of the terrain data should inhibit the development of initially cellular convection, which should subsequently inhibit AEW generation. Exclusion of the Turkana Channel (NTCH) would show the importance of any contribution of flow from the channel to the development of the AEW. Additional cases of AEW development near the EH are also being considered.

6. References

Beven, J., 2000: Tropical cyclone report, Hurricane Alberto, 3-23 August 2000. National Hurricane Center, Miami, FL. (Available at: http://www.nhc.noaa.gov/2000alberto.html)

Burpee, R. W., 1972: The origin and structure of easterly waves in the lower troposphere of North Africa. *J. Atmos. Sci.*, **29**, 77-90.

Carlson, T. N., 1969: Some remarks on African disturbances and their progress over the tropical Atlantic. *Mon. Wea. Rev.*, **97**, 716-726.

Chen, S., J. Cummings, J. Doyle, R. Hodur, T. Holt, C.-S. Liou, M. Liu, J. Ridout, J. Schmidt, W. Thompson, A. Mirin, and G. Sugiyama, 2003: *COAMPS™ version 3 model description: general theory and equations*. NRL/PU/7500—03-448. Naval Research Laboratory, Marine Meteorology Division, Monterey, CA.

Cotton, W. R., M.-S. Lin, R. L. McAnelly, and C. J. Tremback, 1989: A composite model of mesoscale convective complexes. *Mon. Wea. Rev.,* **117**, 765-783.

_______, R. L. George, P. J. Wetzel, and R. L. McAnelly, 1983: A long-lived mesoscale convective complex. Part I: The mountain-generated component. *Mon. Wea. Rev.*, **111**, 1893-1918.

Fritsch, J. M., J. D. Murphy, and J. S. Kain, 1994: Warm core vortex amplification over land. *J. Atmos. Sci.*, **51**, 1780-1807.

Hill, C. M., and Y.-L. Lin, 2003: Initiation of a mesoscale convective complex over the Ethiopian Highlands preceding the genesis of Hurricane Alberto (2000). *Geophys. Res. Lett.*, **30**, 36 (4 pp).

Laing, A. G., and J. M. Fritsch, 2000: The large-scale environment of the global population of mesoscale convective complexes. *Mon. Wea. Rev.*, **128**, 2756-2776.

_______, and _______, 1993: Mesoscale convective complexes in Africa. *Mon. Wea. Rev.*, **121**, 2254-2263.

Lin, Y.-L., N.-H. Lin, and R. P. Weglarz, 1992: Numerical model studies of lee mesolows, mesovortices, and mesocyclones with application to the formation of Taiwan mesolows. *Meteor. Atmos. Phys.*, **49**, 43-67.

_______, K. E. Robertson, and C. M. Hill, 2005: Origin and Propagation of a Disturbance Associated with an African Easterly Wave as a precursor of Hurricane Alberto (2000). *Mon. Wea. Rev*., in press.

Mass, C., 1978: A numerical and observational study of African wave disturbances. Ph.D. dissertation, Univ. of Washington, 277 pp.

Mozer, J. B., and J. A. Zehnder, 1996: Lee vorticity production by large-scale mountain ranges. Part II: a mechanism for the production of African waves. *J. Atmos. Sci.*, **53**, 539-549.

Raymond, D. J., and H. Jiang, 1990: A theory for long-lived convective systems. *J. Atmos. Sci.*, **47**, 3067-3077.

Sun, W.-Y., and J.-D. Chern, 1993: Diurnal variation of lee vortices in Taiwan and the surrounding area. *J. Atmos. Sci.*, **50**, 3404-3430.

Thorncroft, C. D., 1995: An idealized study of African easterly waves. Part III: More realistic basic states. *Quart. J. Roy. Meteor. Soc.*, **121**, 1589-1614.

Trier, S. B., C. A. Davis, and J. Tuttle, 2000: Long-lived mesoconvective vortices and their environment. Part I: Observations from the central United States during the 1998 warm season. *Mon. Wea. Rev.*, **128**, 3376-3395.

_______, _______, and W. C. Skamarock, 2000: Long-lived mesoconvective vortices and their environment. Part II: Induced thermodynamic destabilization in numerical simulations. *Mon. Wea. Rev*., **128**, 3396-3412.

Wegiel, J. W., and C. G. Herbster, 1998: The origin of African easterly waves?. *Preprints, 16th Conference on Weather Forecasting and Analysis.* American Meteorological Society, Phoenix, AZ. 13-15.

Wetzel, P. J., W. R. Cotton, and R. L. McAnelly, 1983: A long-lived mesoscale convective complex. Part II: Evolution and structure of the mature complex. *Mon. Wea. Rev.*, **111**, 1919-1937.

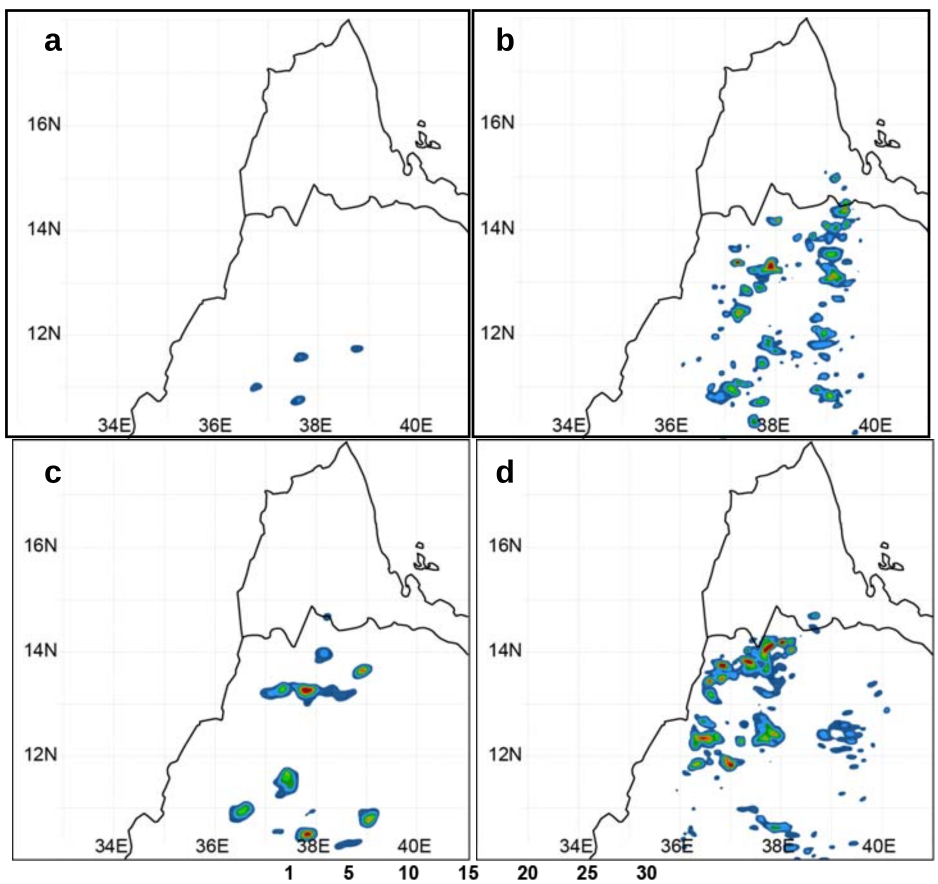

Fig. 3.1. One hour precipitation (mm) field simulated by a) COAMPS at 1200 UTC 28 July 2000, b) MM5 at 1200 UTC 28 July 2000, c) COAMPS at 1600 UTC 28 July 2000, and d) MM5 at 1600 UTC 28 July 2000.

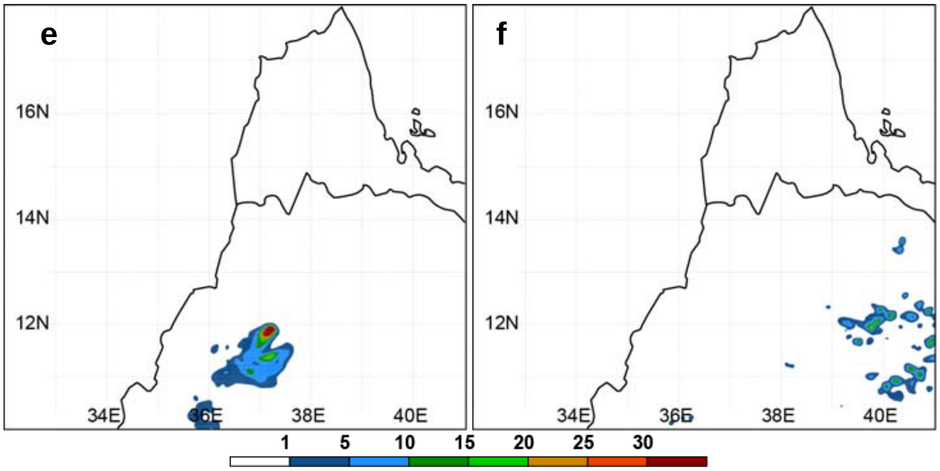

Fig. 3.1. (continued). One hour precipitation field at 2200 UTC 28 July 2000 by e) COAMPS and f) MM5.

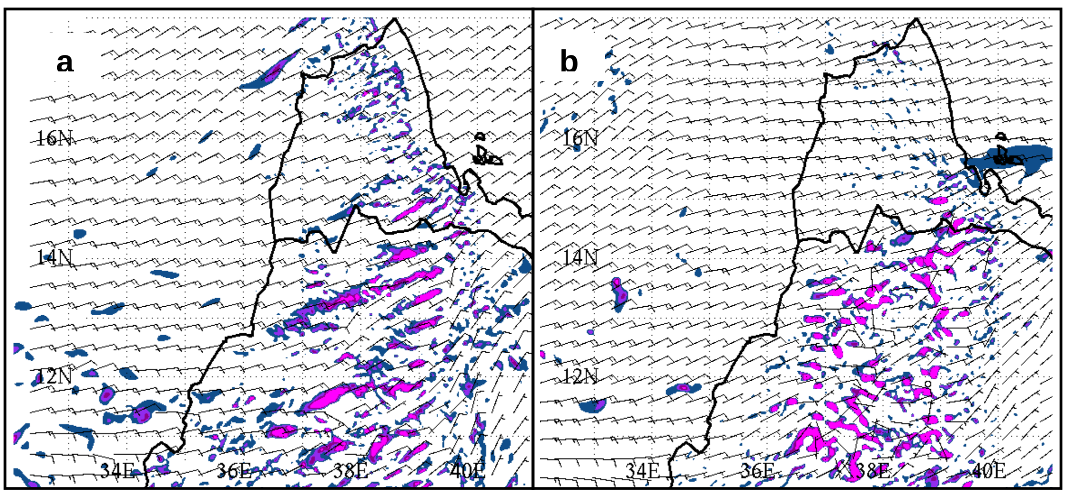

Fig. 3.2. 600-hPa relative vorticity (s-1) and wind (m s^{-1}) at 1200 UTC 28 July 2000 for a) COAMPS and b) MM5. Vorticity is shaded every 10^{-4} s^{-1} up to 4 × 10^{-4} s^{-1}.

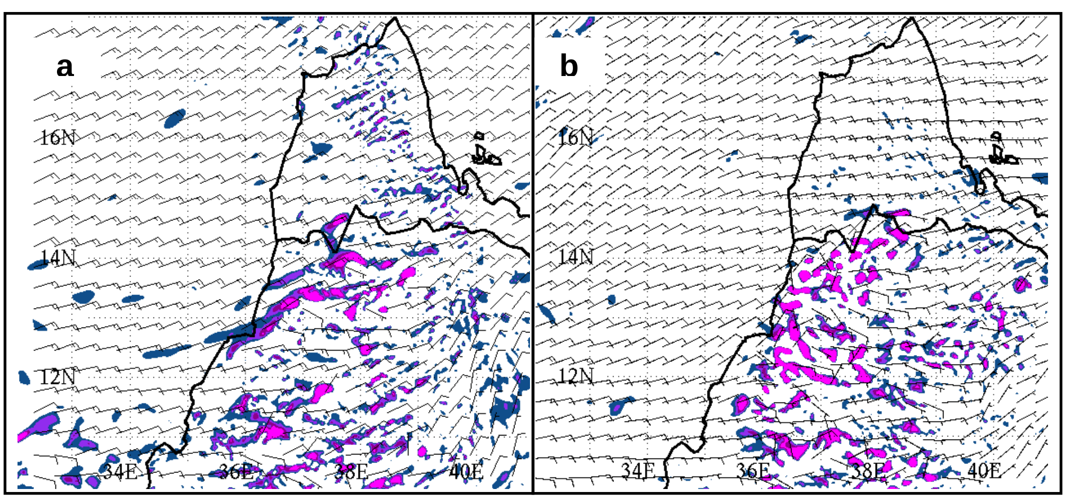

Fig. 3.3. Same as Fig. 3.2, except for 1600 UTC 28 July 2000.

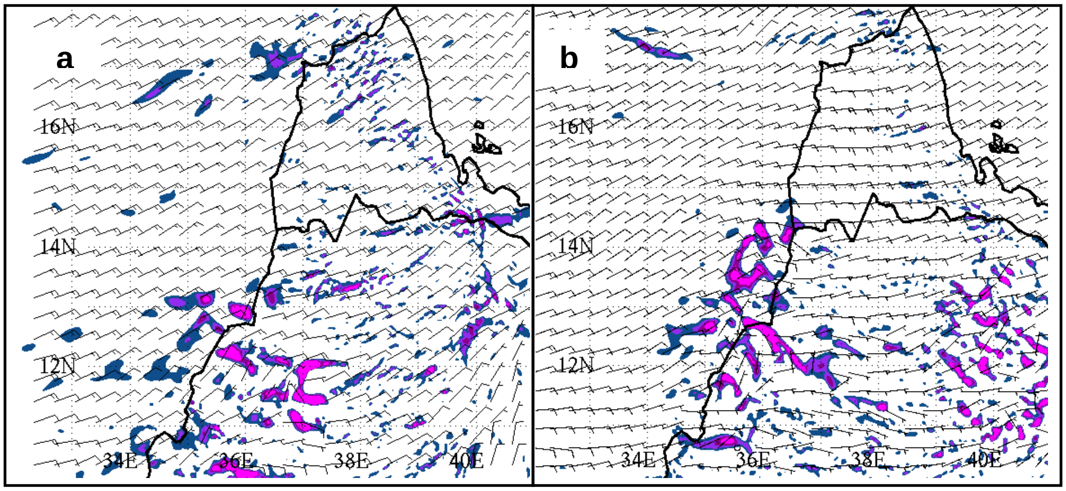

Fig. 3.4. Same as Fig. 3.2, except for 2200 UTC 28 July 2000.

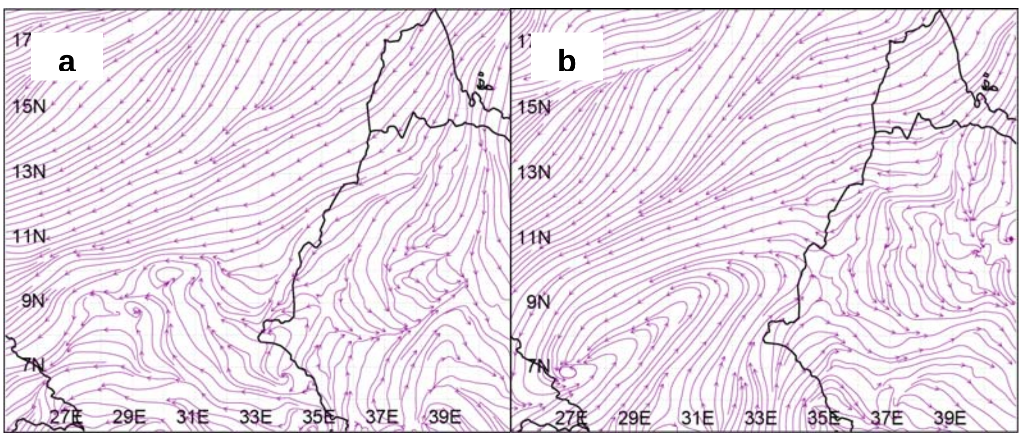

Fig. 3.5. 12-km grid 700-hPa streamline field at 2200 UTC 28 July 2000 for a) COAMPS and b) MM5.

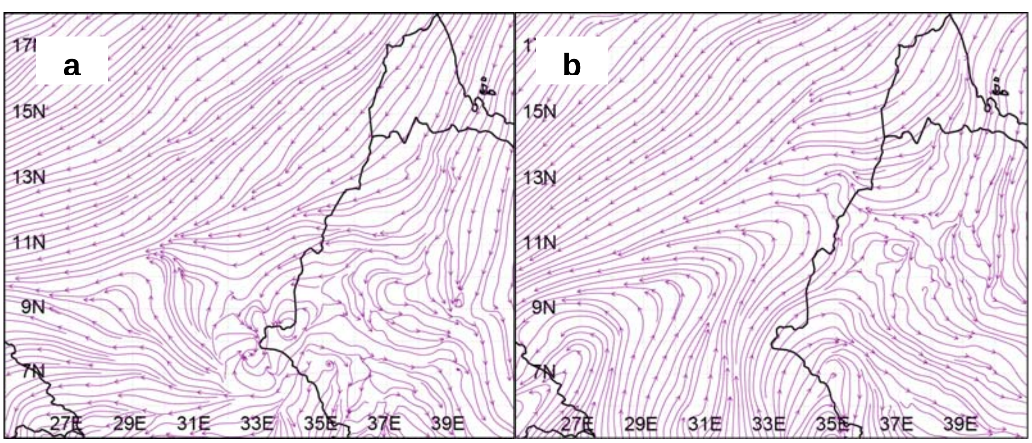

Fig. 3.6. Same as Fig. 3.5, except for 0600 UTC 29 July 2000.

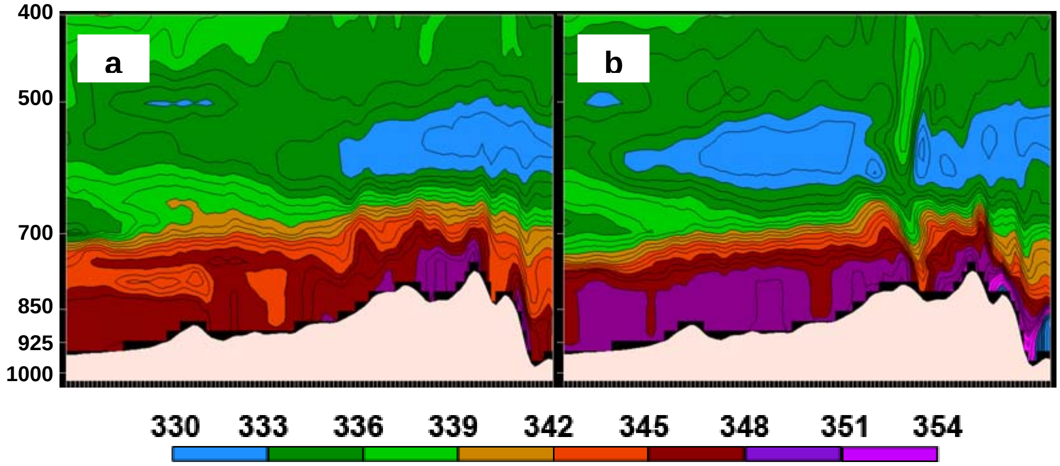

Fig. 3.9. MM5 cross section of equivalent potential temperature along 14.9ºN, and between 36.0ºE and 40.0ºE for a) 0900 UTC 28 July 2000, and b) 1300 UTC 28 July 2000. Contours are every 1 K, and shaded every 3 K.